

ACCEPTED MANUSCRIPT

This is an early electronic version of an as-received manuscript that has been accepted for publication in the Journal of the Serbian Chemical Society but has not yet been subjected to the editing process and publishing procedure applied by the JSCS Editorial Office.

Please cite this article as V. Vahabova, K. Guliyev, and E. Iskenderova, *J. Serb. Chem. Soc.* (2026) <https://doi.org/10.2298/JSC260213023V>

This “raw” version of the manuscript is being provided to the authors and readers for their technical service. It must be stressed that the manuscript still has to be subjected to copyediting, typesetting, English grammar and syntax corrections, professional editing and authors’ review of the galley proof before it is published in its final form. Please note that during these publishing processes, many errors may emerge which could affect the final content of the manuscript and all legal disclaimers applied according to the policies of the Journal.



J. Serb. Chem. Soc. **00(0)** 1-16 (2026)
JSCS-13778

Epoxy- and cyclopropane-functional copolymers: synthesis, thermal properties, and photocrosslinking behavior

VUSALA VAHABOVA*, KAZIM GULIYEV AND ESFIRA ISKENDEROVA

*Institute of Polymer Materials, Ministry of Science and Education of the Azerbaijan Republic,
Sumgait, AZ5004, Azerbaijan.*

(Received 13 February; revised 23 March; accepted 21 April 2026)

Abstract: Copolymers bearing both epoxy and cyclopropane groups were synthesized by free-radical copolymerization of glycidyl 2-(4-vinylphenyl)cyclopropanecarboxylate (GVPCC) with methyl methacrylate (MMA) using AIBN at 343 K, in bulk and in benzene under inert atmosphere. Copolymer compositions were determined by spectroscopy, and copolymerization parameters were evaluated by the Fineman–Ross method. The reactivity ratios were $r_1(\text{GVPCC}) = 0.68 \pm 0.05$ and $r_2(\text{MMA}) = 0.51 \pm 0.07$; their product ($r_1 \cdot r_2 = 0.35$) indicates random copolymerization with a tendency toward alternation. Alfrey–Price parameters ($Q_1 = 0.96$, $e_1 = -0.63$; $Q_2 = 0.74$, $e_2 = 0.40$) confirm strong comonomer interactions and pronounced polar effects. For a 50/50 copolymer, the intrinsic viscosity was 0.66 dL g^{-1} (benzene, 25°C). Thermogravimetric analysis showed composition-dependent stability with $T_5 = 250\text{--}320^\circ\text{C}$, increasing with GVPCC content, alongside improved adhesion (up to 5.6 MPa) and Vicat softening temperature (121°C). UV irradiation produced efficient crosslinking and negative-tone photoresist behavior (resolution with depth of penetration, $D_p = 0.25\text{--}0.35 \mu\text{m}$; critical exposure energy, $E_c = 14.5\text{--}16.4 \text{ mJ cm}^{-2}$; sensitivity, $S = 61\text{--}69 \text{ cm}^2 \text{ J}^{-1}$), demonstrating potential for UV-patternable microfabrication materials.

Keywords: cyclopropane ring; epoxy functionality; UV-induced crosslinking; negative-tone photoresist; working curve.

INTRODUCTION

As modern microelectronic technologies continue to advance, there is a growing demand for new functional polymeric materials with improved performance characteristics. Owing to their high thermal endurance, specific electrophysical properties, and favorable deformation–strength behavior, such

* Corresponding author. E-mail: vusalavahabova@gmail.com
<https://doi.org/10.2298/JSC260213023V>

polymers are widely regarded as indispensable materials for forming protective and insulating layers in the fabrication of microelectronic devices.¹⁻⁶

High-resolution topological patterns in polymer films are typically produced by optical photolithography. In practice, two main strategies are used: either complex multilayer resist systems are employed, or the intrinsic photosensitivity of the polymer is exploited. Introducing built-in photosensitivity into the polymer matrix is considered the more promising approach, since it can significantly simplify processing and enhance the lithographic resolution. However, a persistent limitation remains: most currently available resists exhibit insufficient photosensitivity, which becomes a serious technological bottleneck.

To address this challenge and improve the lithographic performance of negative-tone photoresists, the synthesis of new monomers containing photoactive groups—and the preparation of polymers based on these monomers—remains a highly relevant task. In our earlier studies, the photochemical behavior of difunctionally substituted cyclopropylstyrenes was investigated.⁷ The present work represents a logical continuation of those efforts and is focused on the radical copolymerization of an epoxycarbonyl-substituted cyclopropylstyrene monomer, glycidyl 2-(4-vinylphenyl) cyclopropanecarboxylate (GVPCC), with methyl methacrylate (MMA).

Although the photochemical properties of cyclopropyl-containing styrene derivatives have been explored previously,⁸⁻¹² the combined incorporation of an epoxy functional group together with the cyclopropane fragment—and, importantly, its potential synergistic contribution to photosensitivity—has not been systematically examined. Here, we investigate this effect for the first time.

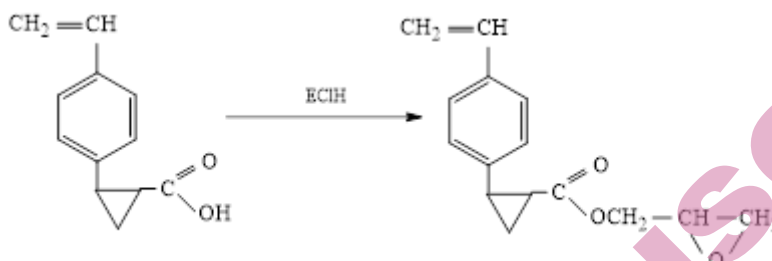
The main objective of this study is to elucidate the copolymerization behavior of GVPCC and to systematically evaluate how the epoxycarbonyl substituent introduced into the cyclopropane fragment of the side chain influences the photosensitivity of the resulting macromolecules. The GVPCC monomer can be considered a promising starting material for producing polymers with properties valuable for microelectronic applications and, consequently, exhibits substantial potential for further practical use.

EXPERIMENTAL

The target monomer, glycidyl 2-(4-vinylphenyl)cyclopropanecarboxylate (GVPCC), was synthesized via the reaction of 2-(4-vinylphenyl)cyclopropanecarboxylic acid with epichlorohydrin (ECH) under basic conditions.

The synthesis was carried out by treating the acid with excess epichlorohydrin in the presence of sodium hydroxide, which facilitated the formation of the glycidyl ester through nucleophilic substitution and subsequent ring closure. The reaction proceeds via the intermediate chlorohydrin, followed by intramolecular cyclization to yield the epoxide-containing monomer.¹³

The overall synthetic route is presented in Scheme 1.



Scheme 1. Synthesis of glycidyl 2-(4-vinylphenyl)cyclopanecarboxylate (GVPCC).

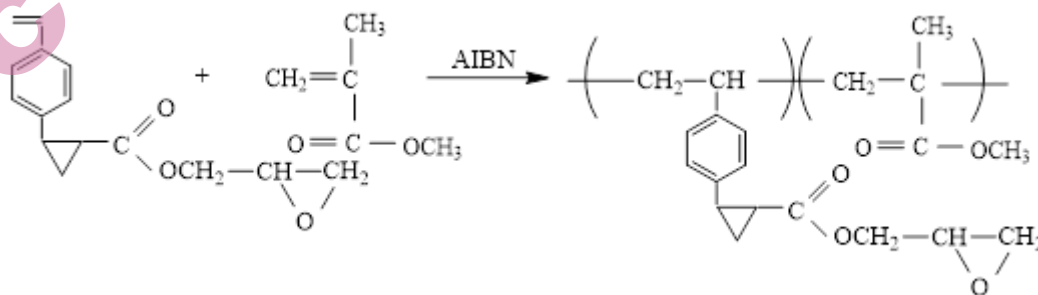
The purity of the monomer was verified by gas chromatography (GC) and was found to be 99.8%.

Copolymerization procedure

To evaluate the reactivity of the synthesized monomer and its potential for practical applications, it was subjected to radical copolymerization with methyl methacrylate (MMA). Methyl methacrylate (MMA, 99%, Sigma-Aldrich) was used as received. The copolymerization of GVPCC with MMA was carried out both in bulk and in benzene solution under a nitrogen atmosphere in sealed glass ampoules.

After mixing the monomers with the initiator (azobisisobutyronitrile AIBN, 98% Sigma-Aldrich was used as received), the reaction mixture was transferred into a glass ampoule. The mixture was purged with nitrogen for 8 min, after which the ampoule was tightly sealed and maintained in a thermostat at 343 K. The initiator concentration was 0.3 wt% relative to the total monomer mass.

The resulting polymer was purified from benzene solution by double reprecipitation into methanol and then dried under vacuum at 30 °C to constant mass at a residual pressure of 15–20 mmHg. Benzene (99.5%, Sigma-Aldrich) and methanol (99.8%, Sigma-Aldrich) were used as received. Yield: 259 mg (83%, based on the total mass of monomers). The intrinsic viscosity of the copolymers was measured in benzene at 25 °C using an Ubbelohde-type viscometer. The radical copolymerization of GVPCC with methyl methacrylate (MMA) initiated by AIBN is shown in Scheme 2.



Scheme 2. AIBN-initiated radical copolymerization of GVPCC with methyl methacrylate (MMA).

Method for evaluating the photosensitivity of the synthesized polymers

Photoresist solutions containing the copolymers (4–13 wt%) were prepared in benzene and spin-coated onto glass substrates at 2500 rpm. Film thickness after drying (room temperature followed by vacuum drying at 50 °C) was 0.20–0.25 μm (Linnik microinterferometer). UV exposure through a photomask was carried out using a DRT/DPT-220 mercury lamp (2.2 A, 15 cm distance, 5–25 s), followed by development in dioxane:isopropyl alcohol (1:2, v/v) at 18–25 °C. Negative-tone behavior was confirmed by the insolubility of exposed areas in the developer. The surface exposure dose was calculated as

$$E_0 = I \cdot t \quad (1)$$

The critical exposure energy (E_c) and penetration depth (D_p) were obtained from the working curve,

$$Cd = D_p \ln(E_0/E_c) \quad (2)$$

where D_p is determined from the slope and E_c from the x-intercept.

RESULTS AND DISCUSSION

Characterization of the copolymers

^1H NMR spectra were recorded on a Bruker AFR-300 spectrometer (300 MHz) in CDCl_3 using tetramethylsilane (TMS) as the internal standard; chemical shifts are reported in ppm (δ) and coupling constants in Hz (J). FT-IR spectra were recorded on a Bruker ALPHA FT-IR spectrometer (Germany). UV-Vis spectra were obtained on a Shimadzu UV-1800 spectrophotometer in the 200–400 nm range. Thermogravimetric analysis (TGA) was performed under nitrogen on a NETZSCH TG 209 F3 Tarsus thermal analyzer at a heating rate of 10 °C min^{-1} .

Adhesion strength was determined by the pull-off method according to ISO 4624 using an Elcometer 510 adhesion tester. Measurements were carried out on polymer films deposited on glass plates at 23 ± 2 °C with a loading rate of 1 MPa s^{-1} . The Vicat softening temperature was determined according to ISO 306 (method B50) using a Vicat softening point apparatus at a heating rate of 50 °C h^{-1} under a load of 50 N. Tensile properties, including tensile strength and elongation at break, were measured on a ИМ-4Р (IM-4R) universal testing machine, AKIM-Metal, Russia in accordance with ISO 527-2 at 23 °C and a crosshead speed of 10 mm min^{-1} . Impact resistance was evaluated by the Charpy method according to GOST 4647 using a MJI-09 pendulum impact tester (Tochpribor, Russia) at room temperature.

The structure of the GVPCC–MMA copolymers synthesized in this work was supported by FTIR and ^1H NMR spectroscopy. In the FTIR spectrum of the GVPCC monomer, the characteristic absorption bands of the vinyl group are clearly observed at 1630 cm^{-1} and 990 cm^{-1} . After polymerization, the vinyl-group bands disappeared in the copolymer, indicating consumption of the double bond, while the intense bands assigned to the cyclopropane ring (1030–1035 cm^{-1}), the ester carbonyl group (1735 cm^{-1}), and the epoxide ring (910 and 1250 cm^{-1}) remain

preserved. The FTIR spectrum of the GVPCC/MMA copolymer is shown in Figure 1.

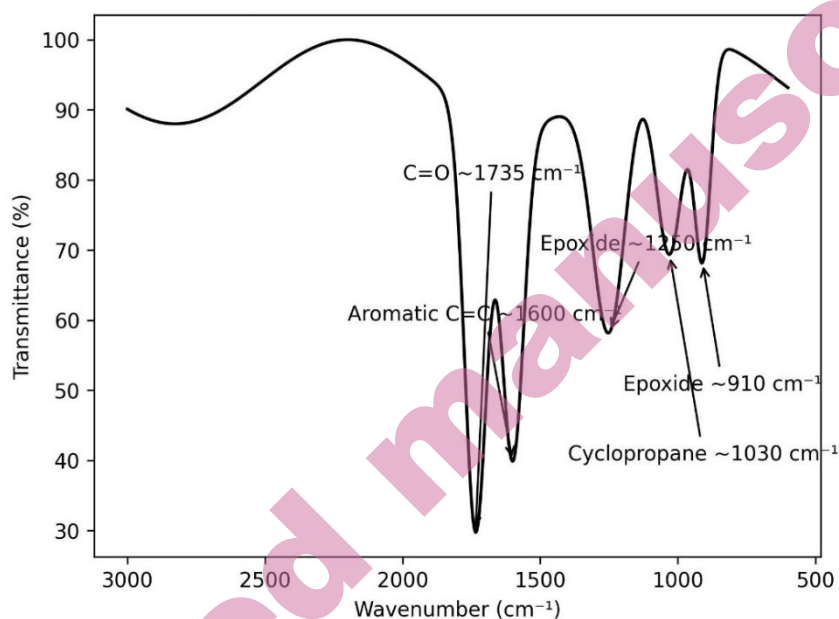


Figure 1. FTIR spectrum of the GVPCC/MMA copolymer.

A similar spectral pattern is observed for the copolymer. However, incorporation of MMA leads to an increase in both the intensity and the breadth of the ester carbonyl (C=O) absorption band in the 1725–1735 cm^{-1} region. This effect can be attributed to the overlap of carbonyl absorptions from two different ester functionalities present in the copolymer structure.

Comparative ^1H NMR analysis

Comparative ^1H NMR analysis was used to determine of the macromolecular composition. In the GVPCC monomer, the vinyl protons give distinct signals in the $\delta= 5.2\text{--}6.7$ ppm region. In the homopolymer, these signals were absent, demonstrating that polymerization proceeds via the vinyl double bond. The ^1H NMR spectrum of the GVPCC–MMA copolymer is shown in Figure 2. The protons of the cyclopropane ring were observed at $\delta= 1.2\text{--}1.8$ ppm, while the epoxide-ring protons were detected in the $\delta= 2.6\text{--}3.2$ ppm range.

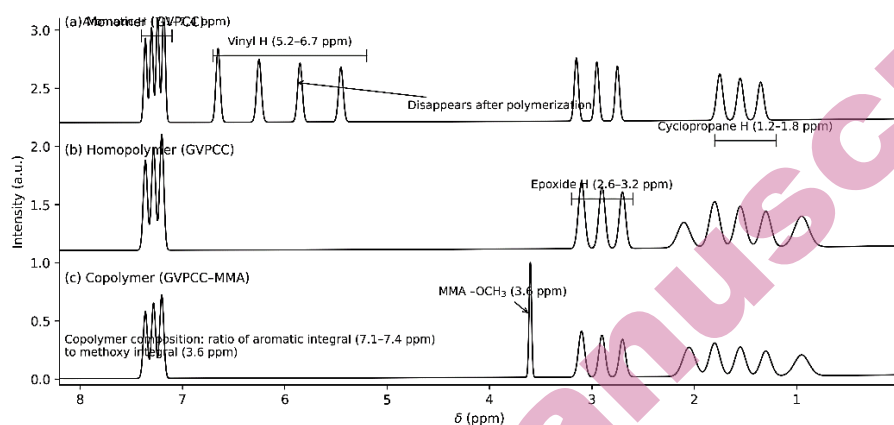


Figure 2. Comparative ^1H NMR spectra of the GVPCC monomer, its homopolymer, and the GVPCC/MMA copolymer (CDCl_3 , 300 MHz).

In the copolymer spectrum, the signals characteristic of the GVPCC-derived units are retained and, in addition, a sharp singlet at $\delta = 3.6$ ppm corresponding to the methoxy ($-\text{OCH}_3$) group of the MMA fragment appears. The molar ratio of the comonomer units in the copolymer was determined from the integral intensity ratio of the aromatic protons of GVPCC ($\delta = 7.1\text{--}7.4$ ppm) to the methoxy protons of MMA.

Copolymer composition and reactivity ratios

Copolymerization was carried out at various initial molar feed ratios of GVPCC and MMA. The composition of the resulting copolymers was determined by ^1H NMR spectroscopy based on the integral intensity ratio of the aromatic protons of the GVPCC units ($\delta = 7.1\text{--}7.4$ ppm) to the methoxy group of MMA ($\delta = 3.6$ ppm). It was found that increasing the fraction of GVPCC in the initial feed led to a proportional increase in the content of epoxycarbonyl and cyclopropane fragments incorporated into the macromolecular chain.

To better understand the copolymerization behavior of the GVPCC/MMA system, the reactions were performed both in bulk and in benzene solution. Bulk polymerization made it possible to assess the behavior of the monomer pair in the absence of solvent, whereas solution polymerization in benzene provided lower viscosity and improved heat transfer, allowing better control of the reaction conditions. The obtained copolymerization results confirmed that GVPCC and MMA undergo efficient copolymerization, as reflected by the reactivity ratios $r_1 = 0.68 \pm 0.05$ and $r_2 = 0.51 \pm 0.07$. Since both values are below unity and the product $r_1 \cdot r_2 = 0.35$, the system shows a tendency toward cross-propagation and partial alternation. Thus, the use of both bulk and solution conditions was helpful for evaluating the effect of the reaction medium on the copolymerization behavior and on the properties of the resulting copolymers.

As a quantitative characteristic of copolymerization, the relative reactivity of the monomers (reactivity ratios) was calculated using the Fineman–Ross method.¹⁴ The compositions of GVPCC (M_1)/MMA (M_2) copolymers obtained at different initial feed ratios were determined by ¹H NMR spectroscopy, and the results are summarized in Table I. The dependence of the copolymer composition on the initial monomer feed was well described by the Mayo–Lewis equation, showing good agreement with the experimental data.

Table I. Copolymer composition for the GVPCC/MMA system

Sample No	M_1 in feed (mol%)	M_2 in feed (mol%)	m_1 in copolymer (mol%)	m_2 in copolymer (mol%)
1	90	10	87.1	12.9
2	75	25	72.2	27.8
3	50	50	52.7	47.3
4	25	75	32.7	67.3
5	10	90	16.1	83.9

Figure 3 illustrates the relationship between the initial monomer feed composition (M_1) and the resulting copolymer composition (m_1) for the GVPCC/MMA copolymerization system. The deviation of the experimental points from the ideal $y=x$ line indicates the occurrence of compositional drift during copolymerization and reflects differences in monomer reactivity during radical chain propagation. At low M_1 values, the fraction of monomer 1 in the copolymer is relatively higher ($m_1 > M_1$), whereas at higher M_1 the data approach the ideal line ($m_1 \approx M_1$). These observations are consistent with reactivity ratios lower than unity ($r_1 < 1$ and $r_2 < 1$) suggesting a preference for cross-propagation in the system and indicating a certain tendency toward alternating incorporation.

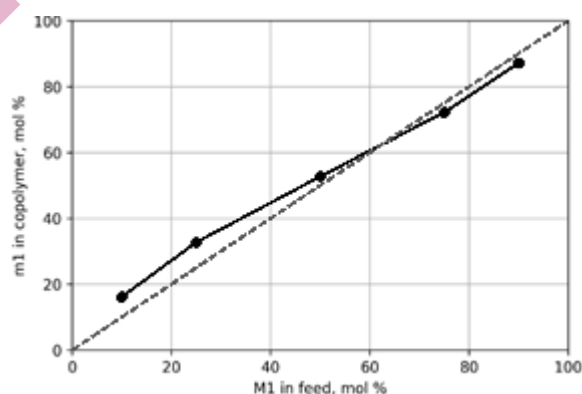


Figure 3. Copolymer composition diagram for GVPCC/MMA: variation of m_1 as a function of the feed fraction M_1 .

Based on the Fineman–Ross analysis, the reactivity ratios were determined as $r_1=0.68\pm 0.05$ for GVPCC and $r_2=0.51\pm 0.07$ for MMA. Since both ratios are below unity ($r_1 < 1$, $r_2 < 1$), each propagating radical preferentially adds the other monomer during chain growth. The fact that $r_1 > r_2$ indicates that the GVPCC-derived radical is more selective than the MMA-derived radical. Moreover, the product $r_1 \cdot r_2 = 0.35$, which is significantly lower than 1, suggests that the copolymerization exhibits a tendency toward alternating incorporation on an otherwise statistical background.

To ensure reliable determination of the reactivity ratios (r_1 and r_2), copolymerization experiments were performed at low conversion (8–10%), and the reactions were quenched at this stage to minimize composition drift.

Copolymer with a GVPCC:MMA feed ratio of 50:50 mol% exhibited an intrinsic viscosity $[\eta]$ of $0.66 \text{ dL}\cdot\text{g}^{-1}$.

To assess the electronic and structural characteristics of the monomers, the Alfrey–Price scheme¹⁶ was applied to determine the Q and e parameters. For the GVPCC/MMA system, the reactivity ratios (r_1 and r_2) obtained at low conversion were used. The literature Q and e values for MMA were treated as fixed constants, and the Q and e parameters of GVPCC were back-calculated using the Alfrey–Price equations. For GVPCC, the values $Q=0.96$ and $e=-0.63$ were obtained.

Compared with the commonly accepted literature values for MMA ($Q=0.74$, $e=0.40$) the higher Q value of GVPCC suggests enhanced resonance stabilization of the vinyl group, promoted by the aromatic ring and the cyclopropane fragment. The negative e parameter (-0.63) reflects the predominance of resonance effects that increase electron density in the monomer. Overall, these results indicate that GVPCC exhibits moderate reactivity and copolymerizes efficiently with MMA. The calculated parameters are summarized in Table II.

Table II. Monomer reactivity ratios and Alfrey–Price Q – e parameters for the GVPCC/MMA copolymerization system.

System	Method	r_1 (GVPCC)	r_2 (MMA)	$r_1 \cdot r_2$	Q_1	e_1	Q_2 (MMA)	e_2 (MMA)
GVPCC/MMA	Fineman–Ross	0.68 ± 0.05	0.51 ± 0.07	0.35		-0.63	0.74	0.40

Note: Q_2 and e_2 values for MMA were taken from the literature; Q_1 and e_1 for GVPCC were back-calculated using the Alfrey–Price scheme and the experimentally determined reactivity ratios.

The thermal behavior of the synthesized GVPCC/MMA copolymers was investigated by thermogravimetric analysis (TGA). The TGA data indicate that thermal degradation proceeds through multiple steps. The initial weight-loss temperature (T_5 , corresponding to 5% mass loss) was observed in the 250–320 °C range depending on the copolymer composition: for GVPCC/MMA = 90/10, $T_5=320^\circ\text{C}$; 75/25, $T_5=305^\circ\text{C}$; 50/50, $T_5=290^\circ\text{C}$; 25/75, $T_5=280^\circ\text{C}$; and 10/90, $T_5=250^\circ\text{C}$ (Figure 4). These results demonstrate that increasing the GVPCC

fraction enhances the thermal stability of the copolymers and confirms that the materials possess sufficiently high thermal resistance for microelectronic processing.

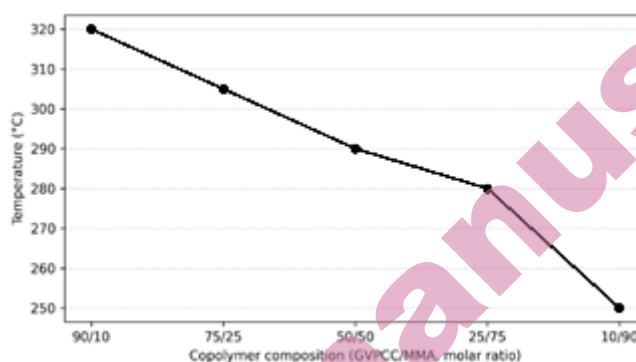


Figure 4. Thermogravimetric (TGA) profiles of GVPCC/MMA copolymers at various GVPCC:MMA ratios.

The observed improvement in stability can be attributed to strengthened intrachain interactions promoted by the cyclopropane ring and aromatic moieties introduced into the side chains, which can hinder bond scission and slow down the overall decomposition process.

Table 3 shows that increasing the GVPCC comonomer content leads to a consistent improvement in both the thermal and mechanical performance of the MMA–GVPCC copolymers. When the GVPCC fraction is increased from 25 mol% to 75 mol%, the adhesion strength rises from 2.5 MPa to 5.6 MPa (approximately a 2.24-fold increase). This enhancement can be directly attributed to the structural features of the GVPCC units: the glycidyl epoxy ring and the ester linkage increase the overall polarity of the copolymer, thereby strengthening interfacial interactions with the substrate—particularly on surfaces bearing polar functional groups—through dipole–dipole interactions and hydrogen bonding. As a result, the interfacial bonding becomes more robust, leading to improved adhesion performance.

The Vicat softening temperature, used here as a measure of heat resistance, is also sensitive to the GVPCC content: 110 °C for 25 mol% GVPCC, 117 °C for 50 mol%, and 121 °C for 75 mol% (an overall increase of 11 °C). This trend can be attributed to the aromatic vinylphenyl fragment and the cyclopropane ring introduced by GVPCC, which restrict segmental chain mobility. As a result, the softening temperature increases and the material exhibits improved dimensional stability at elevated temperatures.

In terms of mechanical performance, the tensile strength increases from 68 MPa to 80 MPa (approximately +12 MPa, ~18%). Importantly, this improvement

is not achieved at the expense of brittleness; on the contrary, the elongation at break rises from 1.8% to 6.9% (about a 3.8-fold increase). These results are consistent with a balanced structure–property effect in the copolymer: rigidifying fragments (aromatic and cyclopropane units) enhance strength, while polar functionalities (ester and epoxy groups) promote local intermolecular interactions, enabling more efficient energy dissipation under deformation.

A similar trend is observed for impact resistance: with increasing GVPCC content, the value rises from 152 to 169 N·cm⁻¹ (an increase of 17 N·cm⁻¹, ~11%). This improvement is consistent with the higher elongation at break and indicates enhanced resistance to damage under dynamic loading.

Overall, the results summarized in Table III demonstrate that increasing the GVPCC fraction leads to a comprehensive enhancement of the MMA–GVPCC copolymer properties: adhesion, heat resistance, strength, ductility, and impact resistance all improve simultaneously. Although the highest performance is achieved for the sample containing 75 mol% GVPCC, a composition of 50 mol% GVPCC may represent a favorable compromise in terms of the heat-resistance–strength–ductility balance, depending on the intended application.

Table III. Effect of GVPCC content (25–75 mol%) in MMA–GVPCC copolymers on adhesion strength, Vicat softening temperature (heat resistance), tensile strength, elongation at break, and impact resistance.

GVPCC content, M ₁ (mol%)	Adhesion strength (MPa)	Vicat softening temp. (°C)	Tensile strength (MPa)	Elongation at break (%)	Impact resistance (N/sm)
25	2.5±0.1	110±2	68±3	1.8±0.2	152±5
50	3.2±0.2	117±2	75±3	4.7±0.3	160±4
75	5.6±0.3	121±2	80±2	6.9±0.4	169±5

Values are given as mean ± standard deviation (n = 3). Overall, the data in Table III show a consistent improvement in adhesion, heat resistance, tensile strength, elongation at break, and impact resistance with increasing GVPCC content.

Increasing the GVPCC fraction leads to a simultaneous rise in strength and elongation at break, suggesting that the “stiffness–ductility” balance in this system cannot be explained solely by chain rigidification. Rather, it is also associated with enhanced intermolecular interactions that promote energy dissipation during deformation. The aromatic ring and cyclopropane fragment within the GVPCC unit restrict segmental rotational freedom and therefore act as rigid structural elements that increase the load-bearing capacity (σ). At the same time, the ester (C=O) and epoxy (C–O) functionalities increase the cohesive energy density of the copolymer and can strengthen dipole–dipole attractions between chains, effectively creating physical association points.

In addition, partial epoxy ring opening under processing conditions (e.g., trace moisture or catalytic impurities) is possible, which would generate –OH groups. In such a case, reversible hydrogen bonds of the –OH···O=C and –OH···O– types may form and act as additional “sacrificial” interactions. These dynamic bonds can delay crack propagation and increase damping of mechanical energy during stretching. The synergistic contribution of dipole–dipole interactions and hydrogen bonding has been reported to improve both strength and toughness (energy absorption/elongation) in various polymer systems.¹⁷

Overall, the rigid fragments introduced by GVPCC (aromatic + cyclopropane) enhance strength, while the polar functionality (ester/epoxy and potentially –OH sites) reinforces dynamic interchain interactions, compensates for embrittlement, and ultimately leads to the balanced mechanical response observed here.

The presence of multiple reactive functionalities of different chemical nature within the synthesized copolymer chains (e.g., epoxy, ether/ester, and cyclopropane fragments) enhances both the photoreactivity of the material and its potential for further functional modification. These groups can facilitate the formation of crosslinks under UV irradiation and may also serve as “active sites” for subsequent amination or other post-polymerization transformations. The synthesized GVPCC/MMA copolymers exhibited efficient UV-induced crosslinking and, according to the insolubility criterion in the developer, showed negative-tone photoresist behavior. A low critical exposure energy (E_c) indicates that network formation can be initiated at a lower energy input, i.e., the material displays high photosensitivity. In this respect, the cyclopropane ring together with the epoxycarbonyl/ester functionalities can be regarded as structural features that promote photochemical conversion and accelerate network formation.

The copolymers also demonstrated high optical transparency ($T \approx 90\%$) which is important for light propagation within the film and for maintaining process stability during photopatterning. In addition, the refractive index $n_p^{20} = 1.583$ can be attributed to the influence of the cyclopropane ring and ester/carbonyl-type groups on polarizability and optical density in the macromolecular environment. Taken together, these characteristics support the potential of the materials as thin-film negative photoresists for applications in microelectronics and optoelectronics.

E_c decreased markedly with increasing copolymer concentration, from ~ 90 mJ cm⁻² at 4 wt% to ~ 15 mJ cm⁻² at 13 wt% (Fig. 5). This trend can be attributed to the higher concentration of photoactive moieties (epoxy and cyclopropane fragments) in the resist film at elevated polymer loadings, which reduces the minimum energy required to initiate network formation under UV irradiation. Such a concentration-dependent decrease in E_c confirms that the resist becomes more sensitive at higher concentrations and can be viewed as a factor that improves energy efficiency in microelectronic photoprocessing, as illustrated in Figure 5.

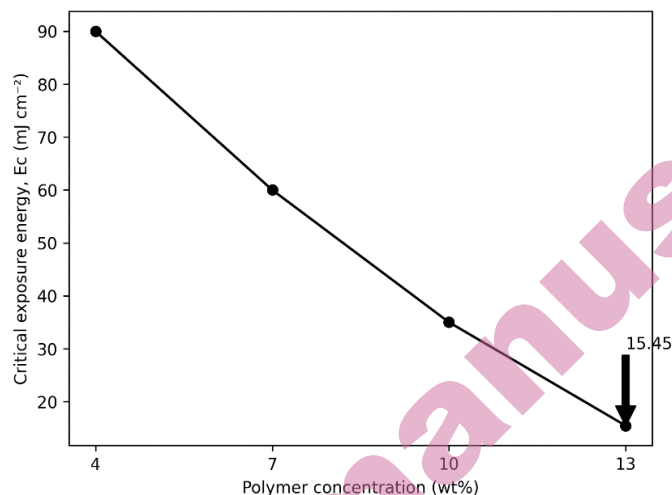


Figure 5. Dependence of the critical exposure energy (E_c) on the concentration of the GVPCC/MMA copolymer (4–13 wt%).

The photoreactive behavior of the synthesized copolymer under UV irradiation was investigated by UV–Vis spectroscopy (Figure 6).

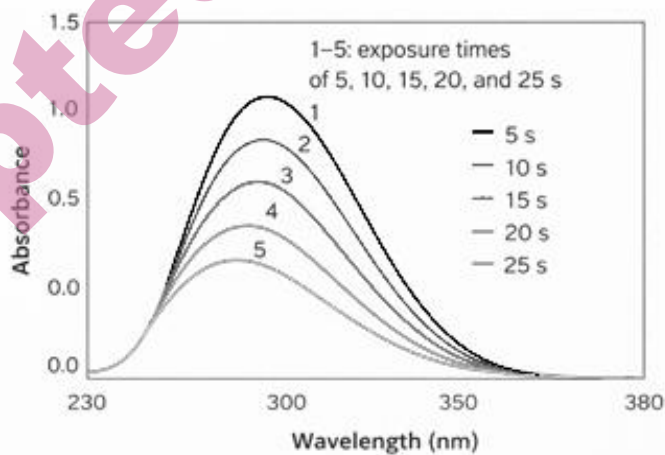


Figure 6. UV–Vis spectra of the GVPCC/MMA copolymer recorded at different exposure times (5, 10, 15, 20, and 25 s), showing the change in absorbance intensity.

UV–Vis spectra showed a progressive decrease of the absorption band at ~296–300 nm as the exposure time increased from 5 to 25 s, indicating consumption of photoactive fragments and advancement of crosslinking. Similar trends have been reported as a sensitive marker of photopolymerization progress.¹⁸ The combined presence of epoxy and cyclopropane units enhances the

photochemical response, which is reflected in the working-curve parameters (E_c and D_p). Under the employed conditions (15 cm distance), 5–25 s exposure was sufficient to obtain stable negative-tone patterns in 0.20–0.25 μm films, as confirmed by optical microscopy.

The measured D_p values (0.25–0.35 μm) are comparable to the film thickness, suggesting that light may penetrate the entire film and cause dose redistribution due to substrate reflection; therefore, thicker films (0.5–1.0 μm) or the use of UV-absorbing additives could improve process robustness. FTIR spectra also support photostructuring, showing a decrease in bands attributed to the epoxide/cyclopropane-related vibrations and the carbonyl group upon irradiation, consistent with network formation. The crosslinking is likely promoted by UV activation of epoxy groups and possible cyclopropane-involving radical processes, resulting in an insoluble 3D network responsible for negative development behavior.

Because the epoxide ring is a highly reactive functional group, it may participate in ring-opening reactions initiated by photo-generated active centers, depending on the formulation and surrounding medium. This interpretation is consistent with the decreased intensity of epoxide-related FTIR bands and supports the assumption that epoxide groups contribute to the crosslinking process. An increased network (gel) density may, in turn, enhance film rigidity and help explain why structuring occurs at relatively low exposure doses (low E_c) in the working-curve analysis (Fig. 7).

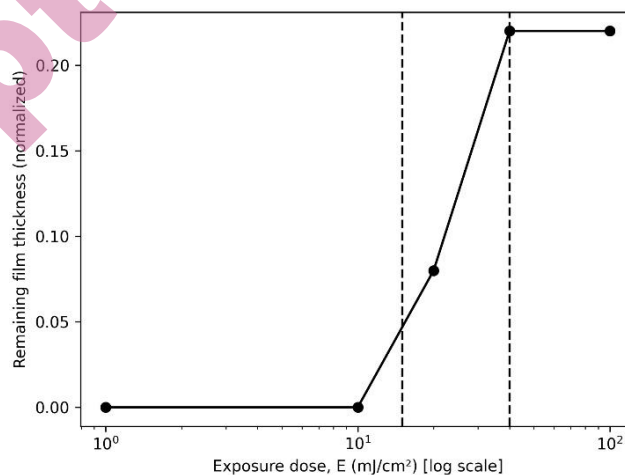


Figure 7. Working curve of the GVPCC/MMA negative-tone photoresist: remaining film thickness after development (d) as a function of exposure dose (E , mJ/cm^2). The critical dose is $E_c = 15.5 \text{ mJ}/\text{cm}^2$, and the effective optical penetration depth is $D_p = 0.25\text{--}0.35 \text{ }\mu\text{m}$ (film thickness: 0.20–0.25 μm).

At the same time, epoxide groups can remain available as reactive sites for amination and other post-polymerization transformations, enabling further post-functionalization of the material.

CONCLUSION

In this work, free-radical copolymerization of the epoxy- and cyclopropane-functional monomer GVPCC with methyl methacrylate (MMA) was carried out, and the composition/structure of the resulting copolymers was confirmed by FTIR and ^1H NMR spectroscopy. Reactivity ratios determined by the Fineman–Ross method were r_1 (GVPCC) = 0.68 ± 0.05 and r_2 (MMA) = 0.51 ± 0.07 ($r_1 \cdot r_2 = 0.35$), indicating that the system exhibits a tendency toward alternating incorporation on a predominantly statistical copolymerization background.

Thermogravimetric analysis showed that the thermal stability of the copolymers depends on composition: the temperature corresponding to 5% mass loss (T_5) ranged from 250 to 320 °C and increased with increasing GVPCC content (e.g., 10/90 \rightarrow 250 °C, 50/50 \rightarrow 290 °C, 90/10 \rightarrow 320 °C). Increasing the GVPCC fraction from 25 to 75 mol% resulted in an overall improvement in both thermal and mechanical performance: adhesion strength increased from 2.5 to 5.6 MPa, and the Vicat softening temperature rose from 110 to 121 °C. At the same time, tensile strength increased from 68 to 80 MPa without a loss in ductility; instead, elongation at break increased from 1.8% to 6.9%, accompanied by an increase in impact resistance from 152 to 169 $\text{N} \cdot \text{cm}^{-1}$.

The copolymers exhibited efficient UV-induced crosslinking and negative-tone photoresist behavior. Working-curve analysis gave $D_p = 0.25\text{--}0.35$ μm and $E_c = 14.5\text{--}16.4$ $\text{mJ} \cdot \text{cm}^{-2}$ ($S = 61\text{--}69$ $\text{cm}^2 \cdot \text{J}^{-1}$), confirming the high photosensitivity of the materials. Overall, combining epoxy and cyclopropane functionality provides a promising functional polymer platform for microelectronic applications, offering improved mechanical/thermal properties together with UV patternability.

Acknowledgements: The experimental work (polymer synthesis and characterization) was carried out at the Institute of Polymer Materials, Ministry of Science and Education of the Republic of Azerbaijan (Sumgayit, Azerbaijan). The authors gratefully acknowledge the Institute for access to instrumentation and laboratory facilities.

ИЗВОД

ЕПОКСИ - И ЦИКЛОПРОПАН-ФУНКЦИОНАЛНИ КОПОЛИМЕРИ: СИНТЕЗА,
ТОПЛОТНА СВОЈСТВА И ПОНАШАЊЕ ПРИ ФОТОУМРЕЖАВАЊУ

VUSALA VANABOVA*, KAZIM GULIYEV и ESFIRA ISKENDEROVA

*Institute of Polymer Materials, Ministry of Science and Education of the Azerbaijan Republic, Sumgait,
AZ5004, Azerbaijan.*

Кополимери са епоксидним и циклопропанским групама синтетизовани су кополимеризацијом глицидил-2-(4-винилфенил)циклопропанкарбоксилата полимеризацијом слободним радикалима (GVPCC) са метил-метакрилатом (ММА) користећи АІВN на 343 К, у маси и бензену под инертном атмосфером. Састави кополимера су одређени спектроскопијом, а параметри кополимеризације су процењени Fineman–Ross методом. Коефицијенти реактивности су били $r_1(\text{GVPCC}) = 0.68 \pm 0.05$ and $r_2(\text{ММА}) = 0.51 \pm 0.07$; њихов производ ($r_1 \cdot r_2 = 0.35$) указује на статистичку кополимеризацију са тенденцијом ка наизменичној. Alfrey–Price параметри ($Q_1 = 0.96$, $e_1 = -0.63$; $Q_2 = 0.74$, $e_2 = 0.40$) потврђују јаке интеракције комономера и изражене поларне ефекте. За 50/50 кополимер, интринстична вискозност је 0.66 dL g^{-1} (бензен, 25 °С). Термогравиметријска анализа показала је стабилност зависну од састава са $T_5 = 250\text{--}320$ °С, која се повећава са GVPCC садржајем, уз побољшану адхезију (до 5.6 МПа) и Викатову температуру омекшавања (121 °С). УВ зрачење је произвело ефикасно умрежавање и понашање фоторезиста негативног тона (резолюција са дубином пенетрације, $D_p = 0.25\text{--}0.35 \mu\text{m}$; критична енергија излагања, $E_c = 14.5\text{--}16.4 \text{ mJ cm}^{-2}$; осетљивост, $S = 61\text{--}69 \text{ cm}^2 \text{ J}^{-1}$), демонстрирајући потенцијал за микрофабрикацију материјала за УВ узорке.

(Примљено 13. фебруара; ревидирано 23. марта; прихваћено 21. априла 2026.)

REFERENCES

1. Q. Lin, *Polymer* **286** (2023) 126395 (<https://doi.org/10.1016/j.polymer.2023.126395>)
2. C. Ober, K. Käfer, F. Yuan, Ch., *Polymer* **280** (2023) 126020 (<https://doi.org/10.1016/j.polymer.2023.126020>)
3. R. Zhou, M. Cao, Y. Tan, M. Neisser, H. Xu, *Sci. Adv.* **11**(29) (2025) 1918 (<https://doi.org/10.1126/sciadv.adx1918>)
4. Y. Wang, H. Yu, L. Wang, Y. Zhang, Z. Zhu, Y. Zhang, Y. Lu, Ch. Ouyang, *J. Mat. Chem. A* **13**(36) (2025) 29860–29884 (<https://doi.org/10.1039/D5TA04194E>)
5. Y. J. Wan, G. Li, Y. M. Yao, X. L. Zeng, P. L. Zhu, R. Sun, *Comp. Comm.* **19** (2020) 154–167 (<https://doi.org/10.1016/j.coco.2020.03.011>)
6. Y. Wen, C. Chen, Y. Ye, Z. Xue, H. Liu, X. Zhou, Y. Zhang, D. Li, X. Xie, Y. Mai, *Adv. Mat.* **34**(52) (2022) e2201023. (<https://doi.org/10.1002/adma.202201023>)
7. K. G. Guliyev, G. Z. Ponomareva, Kh. G. Nazaraliyev, A. M. Guliyev, *Azerb. Khimicheskiy Zhurnal* **1** (1999) 87 (in Russian)
8. K. G. Guliyev, G. Z. Ponomareva, Kh. G. Nazaraliyev, A. M. Guliyev, *Azerb. Khimicheskiy Zhurnal* **1** (1999) 87–90 (in Russian)
9. K.G. Guliyev, S.B. Mamedli, T.S.D. Gulverdashvili, A.M. Guliyev, Book: Applied Chemistry and Chemical Engineering, Imprint: Apple Academic Press., Volume 2, 2017
10. A. I. Sadygova, *Azerbaijan Chem. J.* **3** (2022) 45–50 (<https://akj.az/en/journals/949>)

11. M. Sayes, G. Benoit, A. B. Charette, *Ang. Chem. Int. Ed.* **57** (2018) 13514-13518 (<https://doi.org/10.1002/anie.201807347>)
12. K. Mizuno, N. Ichinose, Y. Yoshimi, J. Photochem. Photobiol. C: Photochem. Rev. **1**(2) (2000) 167-193 ([https://doi.org/10.1016/S1389-5567\(00\)00011-3](https://doi.org/10.1016/S1389-5567(00)00011-3))
13. K.G. Guliev, G.Z. Ponomareva, A. M. Guliev, *Vysokomolekulyarnye soedineniya, Seriya B* **49**(8) (2007) 1577–1581 (*in Russian*)
14. M. Fineman, S. D. Ross, *J. Polymer Sci.* **5** (1950) 259–262 (<https://doi.org/10.1002/pol.1950.120050210>)
15. F. R. Mayo, F. M. Lewis, *J. Am. Chem. Soc.* **66** (1944) 1594–1601 (<https://doi.org/10.1021/ja01237a052>)
16. T. Alfrey Jr., C. C. Price, *J. Polymer Sci.* **2** (1947) 101–106 (<https://doi.org/10.1002/pol.1947.120020112>)
17. Y. Zhang, Y. Li, W. Liu, *Adv. Funct. Mat.* **25**(3) (2015) 471-480 (<https://doi.org/10.1002/adfm.201401989>)
18. J. Bennett, *Addit. Manuf.* **18** (2017) 203–212 (<https://doi.org/10.1016/j.addma.2017.10.009>).